IEEE Access
Multidisciplinary | Rapid Review | Open Access Journal

Received October 20, 2021, accepted November 7, 2021, date of publication November 22, 2021,
date of current version December 3, 2021.

Digital Object Identifier 10.1109/ACCESS.2021.3129849

Predictive Maximum Power Point Tracking for Proton Exchange Membrane Fuel Cell System

JYE YUN FAM[1], SHEN YUONG WONG[2], (Senior Member, IEEE), HAZRUL BIN MOHAMED BASRI[1], (Member, IEEE), MOHAMMAD OMAR ABDULLAH[1], KASUMAWATI BINTI LIAS[1], (Member, IEEE), AND SAAD MEKHILEF[3], (Senior Member, IEEE)

[1]Faculty of Engineering, Universiti Malaysia Sarawak, Kuching, Sarawak 94300, Malaysia
[2]Department of Electrical and Electronics Engineering, Xiamen University Malaysia, Sepang 43900, Malaysia
[3]School of Science, Computing and Engineering Technologies, Swinburne University of Technology, Hawthorn, Melbourne, VIC 3122, Australia

Corresponding author: Shen Yuong Wong (shenyuong.wong@xmu.edu.my)

This work was supported in part by the Xiamen University Malaysia Research Fund under Grant XMUMRF/2021-C8/IECE/0023, and in part by Universiti Malaysia Sarawak.

ABSTRACT This project aims to design a predictive maximum power point tracking (MPPT) for a proton exchange membrane fuel cell system (PEMFC). This predictive MPPT includes the predictive control algorithm of a DC-DC boost converter in the fully functional mathematical modeling of the PEMFC system. The DC-DC boost converter is controlled by the MPPT algorithm and regulates the voltage of the PEMFC to extract the maximum output power. All simulations were performed using MATLAB software to show the power characteristics extracted from the PEMFC system. As a result, the newly designed predictive MPPT algorithm has a fast-tracking of maximum power point (MPP) for different fuel cell (FC) parameters. It is confirmed that the proposed MPPT technique exhibits fast tracking of the MPP locus, outstanding accuracy, and robustness with respect to environmental changes. Furthermore, its MPP tracking time is at least five times faster than that of the particle swarm optimizer with the proportional-integral-derivative controller method.

INDEX TERMS MATLAB, FC, PEMFC, DC-DC boost converter, MPPT.

I. INTRODUCTION

It is well known that the Earth suffers from the depletion of fossil fuels [1]. Thus, there is an urgent need to identify alternative energy sources. Fuel cells (FC) are renewable energy sources that are emerging to deliver clean and efficient power. Its power efficiency can reach 45%, which is higher than that of common electricity generation [2]. Fuel cells can generate electrical power ranging from portable kilowatts to multimegawatt stationary power plants [3]. This technology is applied to residential, commercial, and industrial applications. Therefore, fuel cells can be considered as the top of the desirable technologies for a broad spectrum of power generation applications. This is because it exhibits high efficiency, negligible environmental emissions, and is non-site specific.

Among the fuel cell technologies, proton exchange membrane fuel cells (PEMFCs) have been intensively studied. PEMFCs are the most popular fuel cell types, which use hydrogen gas as fuel. It converts hydrogen and oxygen from chemical to electrical energy. An interesting feature of PEMFCs is their high power density, fast start-up, and low operating temperature [4]. Therefore, it can be used in diverse applications for terrestrial vehicles and rural power plants, but fuel cells require a large investment.

Despite the relatively high efficiency of the fuel cell, the power extracted from the fuel cell is not always optimal because of the ever-changing internal variables [1]. A maximum power point tracking (MPPT) algorithm is required via the power electronics interface to ensure maximum power extraction. The proposed MPPT algorithm modulates the DC-DC power converter to extract the maximum power from the system and guarantee optimal resource usage [5].

II. LITERATURE REVIEW

There are various techniques for MPPT in the literature such as, Perturb and Observe (P&O), Incremental Conductance (IC), Extremum Seeking Control (ESC), Sliding Mode Control (SMC), Fuzzy Logic Control (FLC), Particle Swarm Optimizer (PSO), Radial Basis Function Network (RBFN), and as well, Salp Swarm Algorithm (SSA)

The associate editor coordinating the review of this manuscript and approving it for publication was Zhe Zhang.

methods. The MPPT algorithm has been widely applied to solar photovoltaic (PV) systems to obtain the maximum output power from a PV array. A similar technique can also be used for the fuel cell to determine the maximum power point (MPP) because both systems have similar power curve characteristics.

Naseri *et al.* [6], Dharani and Seyezhai [7], and Dargahi *et al.* [8] introduced a perturb and observe (P&O) approach with a PEMFC to optimize the output power of the fuel cell. This MPPT algorithm compares the rate of change of power and current at each instant according to the step perturbation chosen to generate the maximum power output. This MPPT technique controls the boost converter by regulating the duty cycle and maintains the maximum power of the fuel cell.

Karami *et al.* [1] compared the incremental conductance (IC) and P&O methods for MPPT embedded with FC to enhance the output power with a synchronous DC-DC buck converter. This IC method differentiates the fuel cell power with respect to the current. Then, the maximum power is located at the point when the differentiation result is zero. Both the MPPT efficiencies of the P&O and IC MPPT algorithms are the same. However, IC took less time in MPP tracking, and it was more stable than the P&O method when there were external variations of factors.

Luta and Raji [9] presented and compared fuzzy logic control (FLC) and particle swarm optimizer (PSO)-based MPPT for fuel cell stacks. Both FLC-and PSO-based MPPT techniques control the DC-DC boost controller to extract the maximum power from the fuel cell. The FLC method contains a fuzzy set as a rule consequence to determine the crisp output using the ''Centre of Gravity'' of defuzzification. The concept of PSO is a group communication behavior with a target. This group of organisms represents a potential solution called particles. Each particle has a position with a specified movement to find the best solution. Then, each particle updates the movement based on the previous best position until the best solution can be determined. The results show that the PSO algorithm was better than the FLC controller in terms of convergence time and overshoot problem. On the other hand, FLC performed better in terms of settling time and undershoot problems.

Jiao and Cui [10] and Abdi *et al.* [11] introduced a sliding mode control (SMC)-based MPPT with a DC-DC boost converter for a fuel cell power system. In general, the sliding mode design consists of the design of the sliding surface and the selection of appropriate control law. The sliding function regulates the duty cycle output control. The results show that the SMC approach maintained the maximum output power of the fuel cell, and it was robust to a variety of exterior conditions.

Ahmadi *et al.* [12] improved the PSO-based MPPT using a proportional-integral-derivative (PID) controller. Then, the results are compared with the P&O and SMC methods. The PSO-PID algorithm performed the best from the simulation because it had high accuracy, fast time response, and very low power fluctuations when tracking the maximum powerpoint under variable conditions.

Derbeli *et al.* [13], [14] designed the current estimation MPPT method for PEMFCs based on the estimation of the current reference. The current corresponding to the maximum power point represents the reference current. For different operating temperatures and fuel cell pressures, the reference current can be obtained using the MPP curve. The current reference estimation curve can then be constructed using a fitting function. The backstepping technique regulates the duty cycle of the boost converter. This MPPT method shows satisfactory maximum power point tracking with a fast settling time, high accuracy, and robustness toward external factor variations.

In [15], Derbeli *et al.* also improved the SMC method to a robust high-order SMC based on the ''Twisting Algorithm'' (HOSM-TA). Because of its increased ability to combat the chattering phenomenon and switching control signals, it is an excellent solution for overcoming the disadvantages of traditional SMC. This HOSM-TA is designed to improve the power quality and to maintain the fuel cell operating at an adequate power level. An experiment was conducted to compare the conventional SMC and HOSM-TA methods. From the results, the HOSM-TA method controlled the PEMFC to generate electrical power with a lower power ripple.

Romdlony *et al.* [16] presented an extreme seeking control (ESC) for MPPT with a DC-DC boost converter in a PEMFC system. The ESC traces the MPP of the fuel cell during operation. It traces the MPP subject to fuel cell parameter changes and external loads. Both simulation and experimental results were reported. It can be concluded that extremum-seeking control was effective in tracking the MPP of the fuel cell. However, there was a 9%-10% of ripple in the power generated by the fuel cell.

Reddy and Sudhakar [17] proposed a neural network MPPT controller with a radial basis function network (RBFN) algorithm for a fuel cell system. A three-phase high-voltage gain interleaved boost converter (IBC) was used for electrical vehicle applications. The RBFN consists of three layers: the input, hidden, and output layers. For the fuel cell system, the voltage and current of the fuel cell are the inputs of the RBFN controller, hidden layer as the nonlinear radial basis activation function, and duty cycle of the boost converter as the output. The RBFN-based MPPT was compared with a fuzzy logic controller. The results show that the RBFN-based MPPT controller tracked the MPP of the fuel cell faster than the fuzzy logic controller.

Srinivasan *et al.* [18] also proposed an artificial neural network MPPT controller with a radial basis function network (RBFN) algorithm for PEMFCs. Three different types of DC-DC boost converters were used to compare the maximum power obtained from the PEMFC. These dc-dc boost converters were the boost converters, quadratic boost converters, and reconfigured quadratic boost converters. This research also compared the P&O, FLC, and RBFN-based MPPT methods. From the simulation, MPPT by RBFN extracted the highest power from the PEMFC. On the other hand, the reconfigured

quadratic boost converter performed the best because it converts the highest DC power to the load.

Fathy *et al.* [19] presented a salp swarm algorithm (SSA)-based MPPT for a fuel cell with a PID controller to control the duty cycle of a boost converter. The concept of SSA is that a free-swimming marine leader salp leads its followers to search for the best food at the bottom of the ocean. This SSA with PID-based MPPT was compared with incremental resistance, fuzzy-logic, gray wolf optimizer (GWO-PID), antlion optimizer (ALO-PID), and mine-blast algorithm (MBA-PID) for all studied cases [20], [21]. The results reveal that the SSA-PID extracted the highest MPP from the fuel cell under any operating condition.

The use of model predictive control (MPC) has the advantage of predicting the future behavior of the controlled variables in a model of the system. After that, the controller determines the best actuation based on a predetermined optimization criterion [22]. Pereira *et al.* [23] proposed a neural generalized predictive control (NGPC) for the PEMFC system. A DC-DC boost converter was connected to the PEMFC stack which having the current control loop with a proportional-integral controller. It controlled the current value that was determined by the NGPC algorithm. The NGPC algorithm was designed for both maximum power efficiency and maximum power point tracking. The purpose of using a neural network was to model the non-linear dynamics of the PEMFC so that the efficiency and power predictions can be calculated. The algorithm also involved the cost function minimization which was used to determine the PEMFC output current. During the operation, both the maximum power efficiency and maximum power point were compared. The simulation results show the PEMFC output power for maximum power point tracking algorithm was higher than maximum power efficiency.

Derbeli *et al.* [24] introduced another high-performance tracking method for PEMFC by MPC. This method is not an MPPT but a stable performance tracking technique. It predicts the PEMFC output current for the next two sampling steps. During the operation, a constant reference current represents the PEMFC operational current which is used to calculate the cost function. The best switching combination will be chosen based on the cost function minimization. The results show the MPC tracking method always selected the best switching state. Although this method is not an MPPT method, it proves that the tracking method by MPC maintained the PEMFC output current at the reference current.

An MPPT should be addressed with high priority for the PEMFC system to operate at the highest output power. In this paper, a new predictive MPPT method will be investigated for the PEMFC system to generate the power at MPP. The algorithm of the proposed predictive MPPT technique is different from the method in [23]. However, it is similar to the method in [24] with an MPPT algorithm that can track the MPP. It predicts the PEMFC output current and power for the next sampling step. Then, it compares the PEMFC output power and determines the next switching state without calculating the cost function. Therefore, no reference current is required. The newly designed predictive MPPT method may give prominence to the accuracy and fast-tracking time.

III. METHODOLOGY

This study investigates a predictive MPPT technique for a PEMFC system. This predictive MPPT technique is expected to exhibit fast convergence of the MPP locus, outstanding accuracy, and robustness with respect to environmental changes. The entire simulation is implemented in the MATLAB-SIMULINK environment because this environment is highly flexible in adjusting the operating conditions [25]. First, a fully functional mathematical model of a PEMFC was derived to represent a PEMFC system model. Then, a DC-DC boost converter is designed to control the voltage generated from the PEMFC system. The purpose of controlling the fuel cell voltage is to maintain the fuel cell power at the MPP. A predictive MPPT technique is designed to command to insulated-gate bipolar transistor (IGBT) of the DC-DC boost converter to control the fuel cell voltage. The last step is to validate the newly designed predictive MPPT technique by varying the parameters of the PEMFC system.

A. FULLY FUNCTIONAL MATHEMATICAL MODELING OF PEMFC SYSTEM

The first step is to construct an accurate PEMFC model to simulate the PEMFC system with the MPPT technique. It is essential to study the mathematical modeling and characteristics of PEMFC systems. The fuel cell output characteristics are nonlinear and are affected by the cell temperature, oxygen partial pressure, hydrogen partial pressure, and membrane water content [12], [26]. On the other hand, changes in the load also affect the output power of the PEMFC system.

The energy obtained from the fuel cell is the thermodynamic energy produced from the electrochemical reactions released from the enthalpy of formation, ΔH [27]. This energy can be divided into two thermal energies, which are represented by the Gibbs free energy, ΔG and specific entropy, ΔS in $(kJ\ mol^{-1})$. The Gibbs free energy is affected by changes in the partial pressures of the reactance in a specific volume inside the fuel cell. The equation for this relation can be represented as [14]:

$$\Delta G = \Delta G^{\circ} - RT\left(\ln P_{H_2} + \frac{1}{2}\ln P_{O_2}\right) \tag{1}$$

where $\Delta G^{\circ} = -237.17\ kJ\ mol^{-1}$ is the Gibbs free energy in the standard condition [27], $R = 8.3143\ J\ (mol\ K)^{-1}$ is the gas constant, T is the operational temperature (K) and $F = 96485C$ is the Faraday constant, P_{H_2} and P_{O_2} are the partial pressure of hydrogen and oxygen in (atm), respectively. The potential given by the fuel cell with the effect of changing temperature is defined as [27]:

$$\Delta E = \frac{\Delta S}{nF}\left(T - T_{ref}\right) \tag{2}$$

where $\Delta G = -164\ J\ mol^{-1}K^{-1}$ is the specific entropy, n is the number of electrons released from the anode in the reaction, and $T_{ref} = 298.15°K$ is the standard temperature. For each fuel cell chemical reaction, there are 2 electrons released from the hydrogen gas, so n is equal to 2. Therefore, the electric potential of the cell, also known as the Nernst equation, is given by:

$$E_{Nernst} = -\frac{\Delta G^{\circ}}{nF} + \frac{\Delta S}{nF}\left(T - T_{ref}\right) + \frac{RT}{nF}\ln P_{H_2}P_{O_2}^{0.5} \quad (3)$$

By substituting all the constants into the equation, the Nernst equation can be simplified as:

$$E_{Nernst} = 1.229 - 8.5 \times 10^{-4}\left(T - 298.15\right) + 4.308 \times 10^{-5} T \ln P_{H_2}P_{O_2}^{0.5} \quad (4)$$

The hydrogen and oxygen partial pressures, P_{H_2} and P_{O_2} can be rewritten in the time domain as follows [12]:

$$P_{H_2}(t) = \frac{1}{k_{H_2}}\left(2k_r I_{FC} e^{\left(-\frac{t}{\tau_{H_2}}\right)} + q_{H_2}^{in} - 2k_r I_{FC}\right) \quad (5)$$

$$P_{O_2}(t) = \frac{1}{k_{O_2}}\left(k_r I_{FC} e^{\left(-\frac{t}{\tau_{O_2}}\right)} + q_{O_2}^{in} - k_r I_{FC}\right) \quad (6)$$

where t is the time (s), k_{H_2} and k_{O_2} are the hydrogen and oxygen valve molar constants $(kmol\ atm^{-1}\ s^{-1})$ respectively; $k_r = {}^{N}/_{4F}$ is the modeling constant $(kmol\ s^{-1}\ A^{-1})$, τ_{H_2} and τ_{O_2} are the hydrogen and oxygen time constant (s) respectively; q_{H_2} and q_{O_2} are the molar flow $(kmol^{-1}\ s^{-1})$ of hydrogen and oxygen, respectively.

This Nernst equation is the theoretical reversible thermodynamic potential in (V) and it also represents the open-circuit voltage of the fuel cell [12]. However, in practice, the fuel cell will lose the voltage due to the rate of reactions on the electrodes, the resistance of proton flow in the electrolyte, and the reduction in the concentration of gases. Therefore, the output voltage of a single cell can be defined as:

$$V_{cell} = E_{nerst} - V_{act} - V_{ohm} - V_{conc} \quad (7)$$

where V_{cell} is the output stack voltage (V), V_{act} is the voltage loss (V) due to the rate of reactions on the electrodes, V_{ohm} is the voltage drop (V) from the resistance of proton flow in the electrolyte, V_{con} is the voltage loss (V) from the reduction in the concentration of gases.

The voltage loss at the rate of reactions on the electrodes can be considered as the ignition spark at the beginning of the reaction [27]. Therefore, it is known as the activation overvoltage described by the Tafel equation [12]:

$$V_{act} = \xi_1 + \xi_2 T + \xi_3 T \ln C_{O_2} + \xi_4 T \ln I_{FC} \quad (8)$$

where ξ_1, ξ_2, ξ_3 and ξ_4 are parametric coefficients of the fuel cell model, I_{FC} is the fuel cell output current (A) and C_{O_2} is the concentration of dissolved oxygen $(mol\ cm^{-3})$ on the catalytic interface using the following equation:

$$C_{O_2} = \frac{P_{O_2}}{(5.08 \times 10^6)e^{\frac{-498}{T}}} \quad (9)$$

The voltage loss resistance of proton flow in the electrolyte is known as ohmic overvoltage, which represents the voltage drop due to the resistance of the polymer membrane during proton and electron transfer. The equation is similar to Ohm's law equation, which is defined as:

$$V_{ohm} = I_{FC} R_m \quad (10)$$

where the resistance (Ω) of the electrode R_m can be expressed as

$$R_m = \frac{r_m t_m}{A} \quad (11)$$

From the equation, t_m is the length of the electrolyte (cm) that proton flow, A is the area (cm^2) of the electrolyte that the proton can flow and r_m is the resistivity $(\Omega\ cm)$ of the electrolyte, which can be expressed as [12]:

$$r_m = 181.6\frac{1 + 0.03\left(\frac{I_{FC}}{A}\right) + 0.0062\left(\frac{T}{303}\right)^2\left(\frac{I_{FC}}{A}\right)^{2.5}}{\lambda_m - 0.634 - 3\left(\frac{I_{FC}}{A}\right)e^{4.18\left(\frac{T-303}{T}\right)}} \quad (12)$$

where λ_m is the membrane water content, which varies between 0 and 14. This value represents a relative humidity between 0% and 100%. Under ideal conditions, this parameter may have a value range of 14-20 [10]. The maximum possible value of λ_m can be as high as 23 under supersaturated conditions [28].

The voltage loss from the reduction in the concentration of gases is known as the concentration overvoltage. This voltage drop is due to the concentration gradient of the reactants consumed in the reaction. This equation can be expressed as [12]:

$$V_{con} = -\frac{RT}{nF}\ln\left(1 - \frac{I_{FC}}{i_L A}\right) \quad (13)$$

where i_L is the limiting current density $(A\ cm^{-2})$ of the fuel cell.

Lastly, the output voltage of the fuel cell can be obtained by merging all the equations above. However, the voltage of one cell is very small. Therefore, many cells must be connected to a bipolar plate to increase the output voltage. Therefore, the output voltage (V) of the PEMFC is proportional to the number of cells, N. The equation is given as:

$$V_{FC} = NV_{cell} \quad (14)$$

The output power (W) of PEMFC is defined as:

$$P_{FC} = V_{FC} I_{FC} \quad (15)$$

The fully functional mathematical PEMFC model is programmed in MATLAB software.

B. DC-DC BOOST CONVERTER

Power electronics is a necessary component to track the MPP of PEMFCs because it allows the output voltage to be changed [1]. In this research, a DC-DC boost converter is used to regulate the output voltage of the PEMFC. A DC-DC boost converter is an electronic system used to increase the DC electrical voltage level to a higher level [13]. The relationship between the input and output voltages is controlled by the switch duty cycle, D, using the equation below [13]:

$$V_{out} = \frac{V_{in}}{1 - D} \tag{16}$$

The main components of a DC-DC boost converter are the inductor (L), switch (S), diode (D), and capacitor (C). Figure 1 shows the circuit diagram of the DC-DC boost converter.

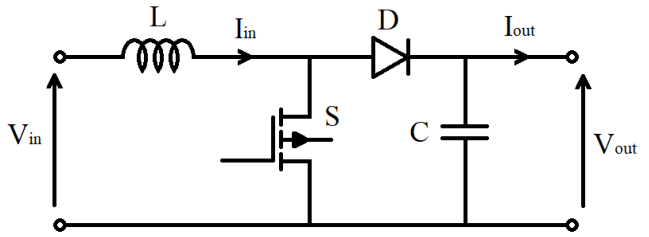

FIGURE 1. DC-DC boost converter.

In this research, the DC-DC boost converter is assumed to be an ideal converter. Therefore, there is no power loss at the diode or switch. By applying Kirchhoff's voltage law, when the switch is OFF, the equation can be described as:

$$S = 0, \quad V_{in}(t) = L\frac{dI_{in}(t)}{dt} + V_{out}(t) \tag{17}$$

When the switch is ON, the equation can be described as:

$$S = 1, \quad V_{in}(t) = L\frac{dI_{in}(t)}{dt} \tag{18}$$

where t is the operation time.

C. PREDICTIVE MPPT TECHNIQUE

The MPPT control process is crucial for achieving good efficiency in a PEMFC power system. From the mathematical modeling of the PEMFC, either the changes in load or the parameter of the fuel cell can significantly affect the output power of the fuel cell. For example, changes in the operational temperature of the fuel cell will result in a change in the MPP of the fuel cell. Figures 2 and 3 shows the V-I and P-I polarization curves of the PEMFC at different operational temperatures.

From Figure 3, the P-I polarization curves show that increasing the operating temperature will increase the MPP of the PEMFC. For different MPPs, the maximum power voltage and current are also different. Therefore, MPPT control is necessary to force the PEMFC system to generate the highest output power under all conditions. The P-I polarization curve of PEMFC has a similar shape to the P-V polarization curve

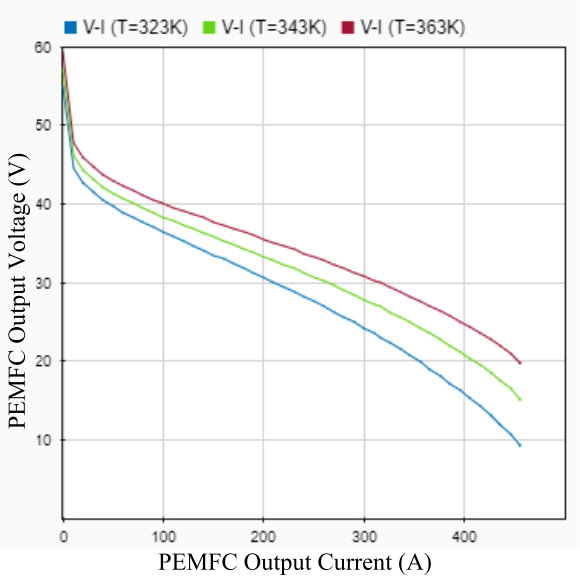

FIGURE 2. PEMFC V-I polarization curve with different operation temperature.

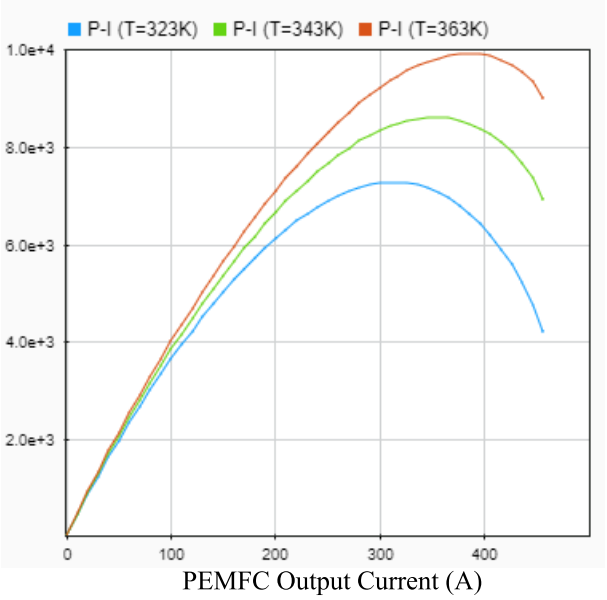

FIGURE 3. PEMFC P-I polarization curve with different operation temperature.

of the solar panel. The existing MPPT methods such as P&O and IC can track the MPP for PEMFC and solar panels. However, these methods do not have outstanding performance in accuracy and tracking time. The proposed predictive MPPT technique is only specialized for PEMFC. For every sampling step, it reads the parameter of the PEMFC such as operational temperature, membrane water content, and partial pressure of reactant gases. This is because different parameters give different MPPs. The predictive MPPT algorithm involves the parameters of the PEMFC in the calculation to select the best switching state for the DC-DC boost converter.

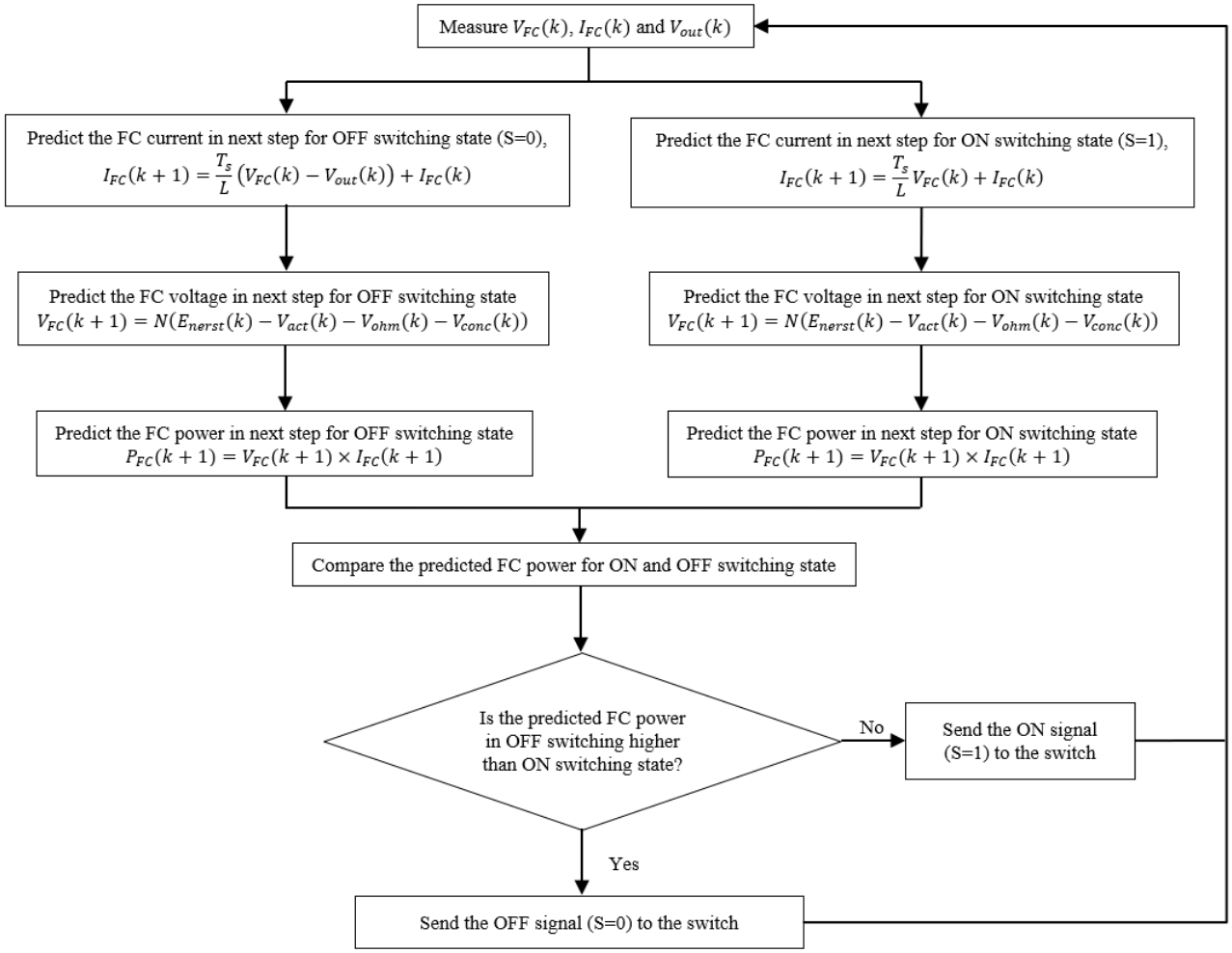

FIGURE 4. Predictive MPPT method flow chart for PEMFC system.

In this study, a predictive MPPT technique was designed and applied to the PEMFC system. The MPPT algorithm is required to work together with the DC-DC boost converter. The MPPT algorithm controls the switch of the boost converter and regulates the output voltage of the fuel cell to a maximum power voltage. The relationship between the fuel cell output voltage, converter input, and output voltage needs to be defined first to develop the predictive MPPT algorithm. When the DC-DC boost converter is connected to the PEMFC, the output voltage of the fuel cell becomes the input voltage of the DC-DC boost converter. Therefore, the equations can be simplified as:

$$S = 0, \quad V_{FC}(t) = L\frac{dI_{FC}(t)}{dt} + V_{out}(t) \tag{19}$$

$$S = 1, \quad V_{FC}(t) = L\frac{dI_{FC}(t)}{dt} \tag{20}$$

Then, the final equation can be concluded as:

$$V_{FC}(t) = L\frac{dI_{FC}(t)}{dt} + \bar{S}V_{out}(t) \tag{21}$$

This predictive MPPT technique involves the model predictive control (MPC) strategy in the DC-DC boost converter introduced in [29]. The critical feature of MPC is the prediction of the future behavior of the controlled variables [22]. Therefore, the equation must be expressed as a discrete-time model. Then, the predictive MPPT algorithm can calculate the fuel cell output voltage and current in the next sampling step. Thus, a one-step prediction of fuel cell power can be computed. In a discrete-time model, the predicted fuel cell current can be expressed as:

$$I_{FC}(k+1) = \frac{T_s}{L}\left(V_{FC}(k) - \bar{S}V_{out}(k)\right) + I_{FC}(k) \tag{22}$$

where k is the number of discrete sampling steps and T_s is the sampling time. This equation includes two conditions: ON switching state and OFF switching state. Therefore, two predicted fuel cell currents were calculated under both conditions.

After the fuel cell currents are predicted in both switching states, the predicted fuel cell voltages can also be calculated by substituting the predicted current into (4)-(14). The fuel

TABLE 1. PEMFC system parameters.

MPPT Methods	Advantages	Disadvantages	Reference
Perturb and Observe (P&O)	• Low complexity	• Slow convergence speed of MPP • Low stability • High power ripple	[6]–[8]
Incremental Conductance (IC)	• Low complexity	• Slow convergence speed of MPP • Low stability	[1]
Fuzzy Logic Control (FLC)	• Fast convergence speed of MPP • High stability	• High complexity • High power ripple	[9]
Particle Swarm Optimizer (PSO)	• Fast convergence speed of MPP • High stability	• High complexity • High computational burden • High power ripple	[9]
PSO with Proportional-Integral-Derivative (PID)	• Fast convergence speed of MPP • High stability • Low power ripple	• High complexity • High computational burden	[12]
Sliding Mode Control (SMC)	• Fast convergence speed of MPP • High stability	• High complexity • High power ripple	[10]–[12]
High-Order SMC based on the "Twisting Algorithm" (HOSM-TA)	• Fast convergence speed of MPP • High stability • Low power ripple	• High complexity	[15]
Current Estimation	• Low complexity • Low power ripple	• Slow convergence speed of MPP	[13], [14]
Extreme Seeking Control (ESC)	• Low complexity	• Slow convergence speed of MPP • High power ripple	[16]
Radial Basis Function Network (RBFN)	• Fast convergence speed of MPP	• High complexity • High power ripple	[17], [18]
Salp Swarm Algorithm (SSA) with PID	• Fast convergence speed of MPP • High stability • Low power ripple	• High complexity • High computational burden	[19]
Neural Generalized Predictive Control (NGPC)	• High stability • Low power ripple	• Slow convergence speed of MPP	[23]
Model Predictive Control	• High stability • Low complexity	• Slow convergence speed of MPP	[24]

cell power for the ON and OFF switching states can be computed by multiplying the predicted current and voltage in the ON and OFF switching states, respectively. The last step of the predictive MPPT is to compare the fuel cell power in both switching states and determine the switching state with higher output power. Once the MPPT algorithm determines the switching state, it sends a signal to control the switch of the boost converter. Therefore, the switch will either switch ON or OFF based on the command given by the MPPT controller. Finally, the boost converter regulates the output voltage of the fuel cell and maintains the maximum output power.

Figure 4 shows a flowchart of the predictive MPPT technique used in the PEMFC system. The MPPT control process is described in the flowchart step by step.

D. MODELING OF PEMFC SYSTEM

Because fully functional mathematical modeling of the PEMFC system, dc-dc boost converter, and predictive MPPT control are designed, the entire PEMFC system with MPPT control can be constructed. The DC-DC boost converter is the main power electronic that is connected between the PEMFC system and the load. The predictive MPPT controller is directly connected to the switch of the DC-DC boost converter and manipulates the switching state. Therefore, the output voltage of the fuel cell is regulated by the DC-DC boost converter according to the MPPT algorithm. Figure 5 shows the configuration of the PEMFC system with the predictive MPPT controller.

IV. SIMULATION RESULTS AND DISCUSSION

In this research, the entire simulation is performed using MATLAB/Simulink. As mentioned in (4)-(15), the fuel cell parameters significantly affect the output voltage, current, and power. The parameters of PEMFC are set and tabulated in Table 2.

The proposed MPPT technique is simulated on the PEMFC system using the parameters listed in Table 2. The simulations are divided into several cases. The first case is to simulate the proposed MPPT on the PEMFC system with the exact value of the fuel cell parameters listed in Table 1. Then, the simulations are proceeded with varying operational temperature and membrane water content to validate the robustness of the MPPT technique. Finally, the proposed MPPT technique is validated by changing the load resistance.

A. SIMULATION WITH CONSTANT OPERATIONAL TEMPERATURE AND MEMBRANE WATER CONTENT

In Table 2, the operational temperature and membrane water content were 343 K and 14, respectively. In Figure 6, the P-I

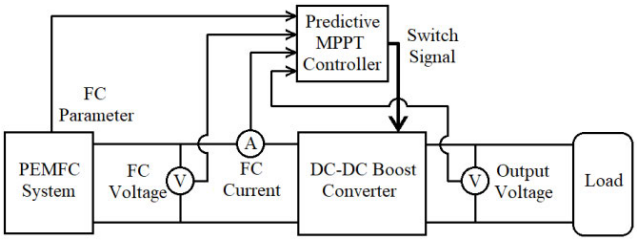

FIGURE 5. PEMFC system and predictive MPPT controller configuration.

TABLE 2. PEMFC system parameters.

Parameter	Symbol & Unit	Value
Temperature	$T\ (K)$	343
Membrane Water Content	λ_m	14
Number of Cells	N	35
Active Area	$A\ (cm^2)$	232
Hydrogen valve molar constant	$k_{H_2}\ (kmol\ atm^{-1}\ s^{-1})$	4.22×10^{-5}
Oxygen valve molar constant	$k_{O_2}\ (kmol\ atm^{-1}\ s^{-1})$	2.11×10^{-5}
Hydrogen time constant	$\tau_{H_2}\ (s)$	3.37
Oxygen time constant	$\tau_{O_2}\ (s)$	6.74
Hydrogen input flow	$q_{H_2}\ (kmol\ s^{-1})$	10×10^{-5}
Oxygen input flow	$q_{O_2}\ (kmol\ s^{-1})$	5×10^{-5}
Membrane thickness	$t_m\ (cm)$	0.0178
Coefficient 1	ξ_1	0.944
Coefficient 2	ξ_2	-0.00354
Coefficient 3	ξ_3	-7.8×10^{-8}
Coefficient 4	ξ_4	1.96×10^{-4}
Limiting current density	$i_L\ (A\ cm^{-2})$	2
Load resistance	$R_L\ (\Omega)$	10

curve shows that the maximum fuel cell output power generated is 8628 W with a current of 355.6 A. Therefore, after the predictive MPPT controller is applied to the PEMFC system, the output power of the fuel cell should be approached to 8628 W. Figure 6 shows the simulation results of the output voltage, current, and power of the fuel cell.

From the simulation results, the FC output power achieves 8628 W within 0.015 s after starting the operation. This FC power curve resembles a first-order system with zero overshoot. At the same time, the fuel cell achieves an output voltage of 24.27 V and current 355.6 A. This output voltage is the maximum power voltage regulated by the DC-DC boost converter to achieve the highest power that can be extracted from the fuel cell. However, the output power of the fuel cell is decreased slowly with time.

This is because the partial pressures of hydrogen and oxygen also decreased with time during the operation. From equation (5), the initial partial pressure of hydrogen is $q^{in}_{H_2}/k_{H_2}$, which is decreased by $2k_rI_{FC} - 2k_rI_{FC}e^{\left(-\frac{t}{\tau_{H_2}}\right)}/k_{H_2}$ with time. After a period, the final partial pressure of hydrogen becomes $q^{in}_{H_2} - 2k_rI_{FC}/k_{H_2}$. The same occurrence occurs for the partial pressure of oxygen, which decreases with time, as shown in (6). This phenomenon was proven in [12] using

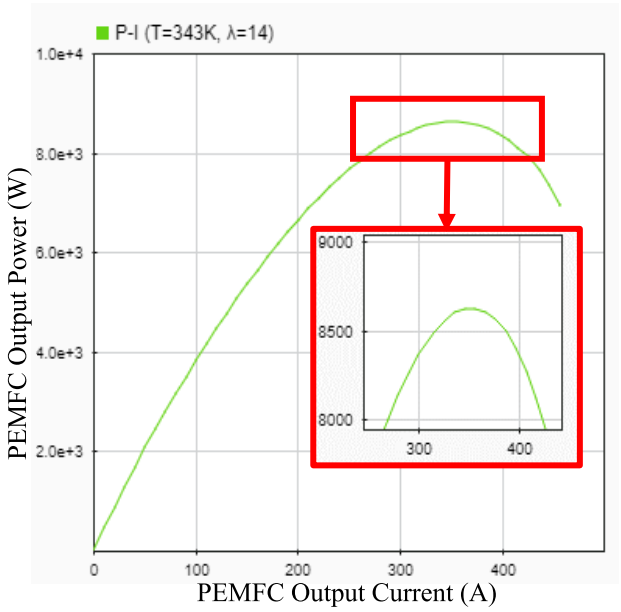

FIGURE 6. P-I characteristic of PEMFC (T = 343K, λ_m = 14).

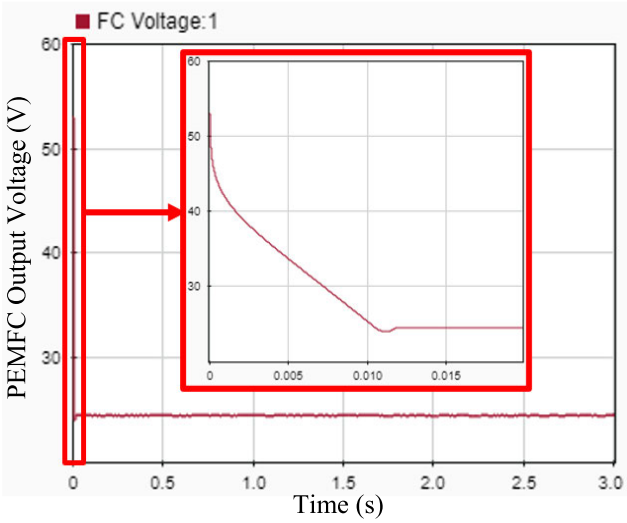

FIGURE 7. PEMFC output voltage for constant fuel cell parameter.

a graph. Figure 10 shows the PEMFC P-I polarization curve with different partial pressures of reactance gases.

In Figure 10, higher partial pressure of reactance gases results in a higher MPP. During fuel cell operation, the partial pressure of the reactance gases is decreased with time. This causes the MPP to move to a lower position with different voltages and currents.

The proposed MPPT technique has a very fast tracking time. The simulation results are compared with the results in [12] to evaluate the performance of the proposed MPPT technique. In [12], the proposed PSO-based MPPT is a proportional-integral-derivative (PID) controller, which was compared with the P&O and SMC techniques. The results in [12] proved that the PSO-PID method had the fastest MPP

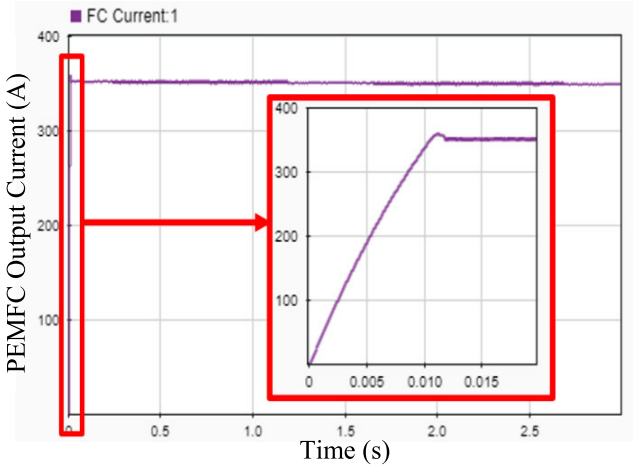

FIGURE 8. PEMFC output current for constant fuel cell parameter.

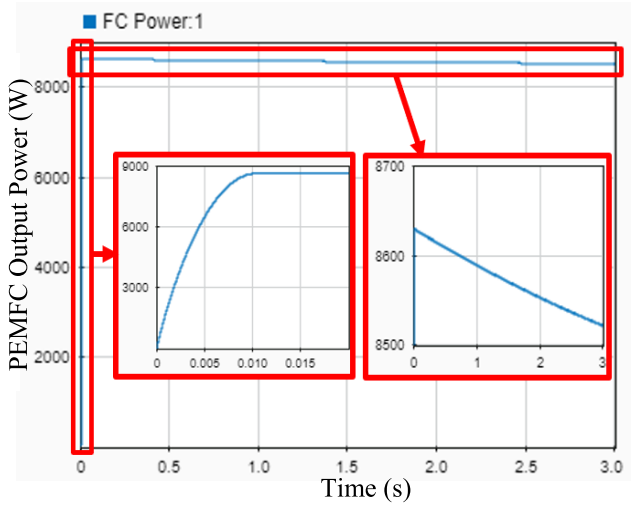

FIGURE 9. PEMFC output power for constant fuel cell parameter.

TABLE 3. MPPT technique comparison.

MPPT Technique	MPPT Accuracy	Settling Time
Predictive MPPT (proposed)	99.13%	0.012s
PSO-PID	98.65%	0.070s
SMC	98.32%	0.100s
P&O	97.82%	0.900s

tracking time. Table 3 shows a comparison of the proposed predictive MPPT method with the PSO-PID, P&O, and SMC techniques in [12].

Table 3 shows the fuel cell achieved the maximum power current within 0.07 s when using the PSO-PID method. However, the proposed predictive MPPT technique can achieve a maximum output power within 0.012 s. Its MPP tracking time is at least five times faster than the PSO-PID method. If the MPP tracking time is fast, less time taken is required to achieve the PEMFC power at MPP. It reflects less energy loss because the power extracted from the PEMFC achieving

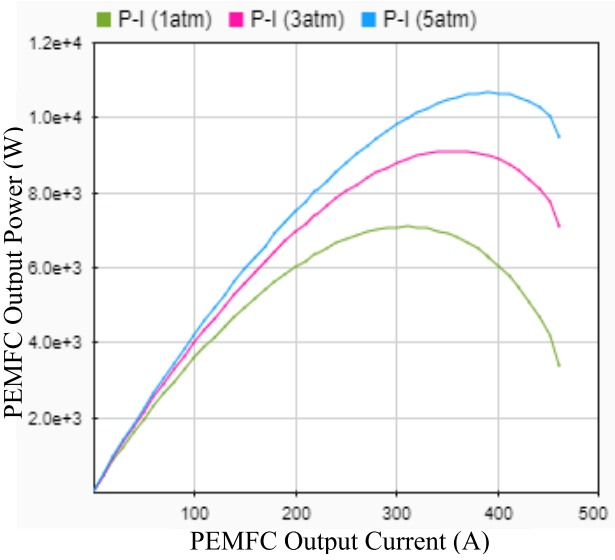

FIGURE 10. PEMFC P-I polarization curve with different partial pressure of reactance gases.

the MPP is fast. In addition, the proposed predictive MPPT technique has the highest tracking accuracy, which achieves 99.13% of the maximum power. It extracts the highest output power from the PEMFC. Therefore, the proposed MPPT technique performs best in terms of MPP tracking accuracy and tracking time.

The proposed predictive MPPT technique has the advantage of having the fastest MPP tracking time with the highest maximum power extracted from the PEMFC system. The predictive MPPT technique can predict the power extracted from the PEMFC in the next step. Then, it selects the best switching state so that the DC-DC boost converter can regulate the DC voltage to the maximum power voltage. Switching state selections are straightforward and do not require iterative calculation. Thus, the predictive MPPT controller will always command the PEMFC system to generate higher electrical power within a very short time.

Another difference between the predictive MPPT technique and the existing MPPT technique is that the existing MPPT technique always regulates the duty cycle of the DC-DC boost converter to maintain the power of the fuel cell at its maximum. However, the predictive MPPT technique determines the switching state of the switch in the DC-DC boost converter. At each sampling time, the predictive MPPT controller can send a signal to change the switching state. Therefore, the switching state is not constrained by the duty cycle. This shows the advantage of having fewer power oscillations and ripples. The shorter the sampling time, the smaller the ripples produced. Therefore, a very small sampling time may result in negligible ripple. This advantage also led to a faster MPP tracking time. Figure 11 shows the switching state selected by the predictive MPPT algorithm.

From the operation time 0 s to 0.012 s, there are two switching cycles to track the MPP. For a conventional

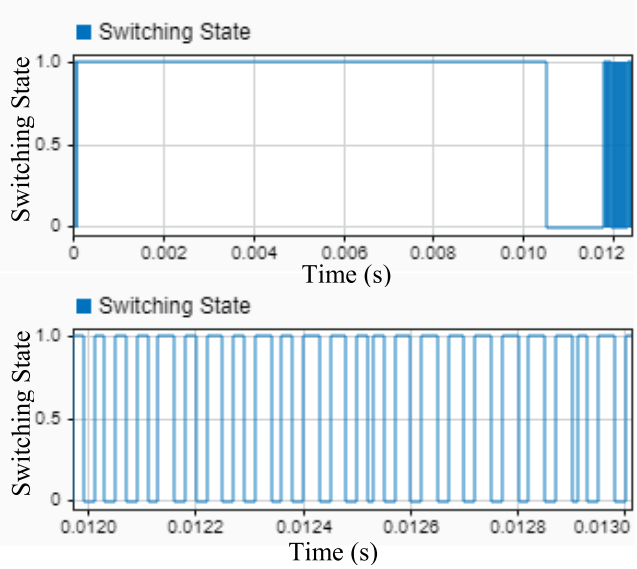

FIGURE 11. Switching state controlled by predictive MPPT algorithm.

dc-dc boost converter, the inductor stores the energy when the switch is switched ON and it releases the energy when the switch is switched OFF. When the operation is started, the switch is switched ON for a period to increase the PEMFC output current until it achieves the current at MPP. At the same time, the energy is stored in the inductor. After that, the switch of the boost converter starts to switch ON and OFF continuously. The inductor will store or release the energy adequately and maintains the PEMFC output current at MPP current. The power extracted from the PEMFC will be the maximum power if the current is kept at MPP.

Figure 11 also shows the switching cycle from 0.012 s to 0.013 s is 23. It means that the switching frequency is around 23 kHz. In [30], an experiment analysis for the conventional DC-DC boost converter is carried out by using a metal-oxide-semiconductor field-effect transistor (MOSFET) as the switch. The switching frequency is set to be 100 kHz which is much higher than the switching frequency in Figure 11. Most of the MOSFET and IGBT available in the market can handle the switching frequency at 23 kHz. Therefore, the issue of temperature rises will not occur. In the market, there is an IGBT named SKM800GA176D, which can handle the current as high as 830 A. It is suitable to be applied as the switch in the boost converter for the PEMFC system. Even though there are spike occurred in a short time, the IGBT will not be damaged.

For the existing MPPT technique, the algorithm does not have a predictive function. Instead, it regulates the duty cycle of the DC-DC boost converter based on the present situation. Moreover, because its algorithm regulates the duty cycle, it requires more time for the oscillation to become stable. In addition, existing MPPT techniques may require more iterations to track the MPP. Therefore, the proposed predictive MPPT has the best performance compared to the MPPT technique in [12].

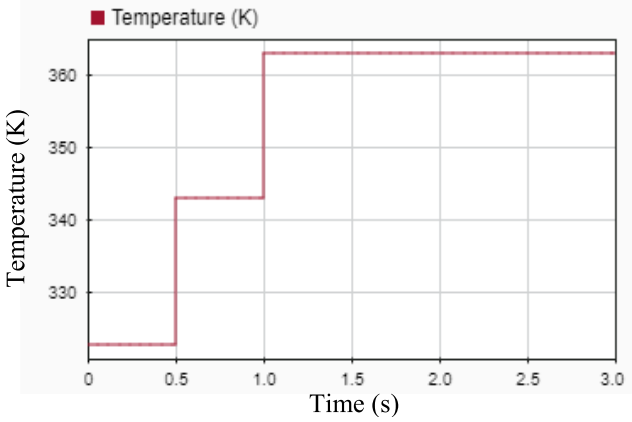

FIGURE 12. Time variations of operating temperature.

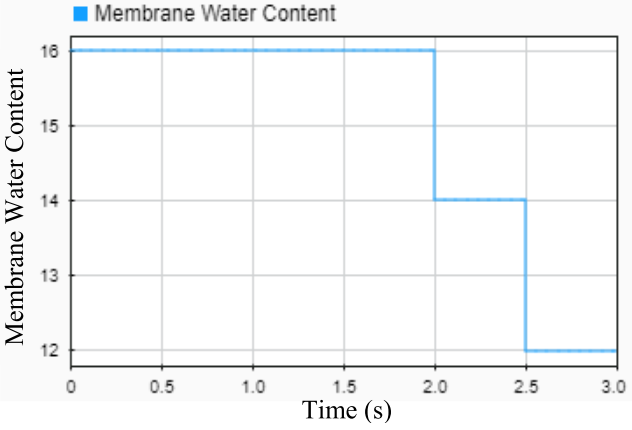

FIGURE 13. Time variations of operating membrane water content.

B. SIMULATION WITH VARIABLE OPERATIONAL TEMPERATURE AND MEMBRANE WATER CONTENT

The simulation is also performed under fast variations of the operational temperature and membrane water content to validate the performance of the proposed MPPT technique under varying parameters. In this simulation, the initial operating temperature is set to be 323 K, and the membrane water content is set to be 16. The operating temperature increases from 323 K to 343 K and then to 363 K in the first 1.5 seconds. After that, the membrane water content decreased from 16 to 14 and then to 12 in the last 1.5 seconds. Figures 12 and 13 show the time variations of the operational temperature and membrane water content during operation in this simulation.

Figure 14 shows the P-I polarization curves with constant membrane water content but different operational temperatures. When the operating temperatures are 323 K, 343 K, and 363 K at a constant membrane water content ($\lambda = 16$), the maximum power points of the fuel cell are 8154 W, 9601 W, and 10970 W, respectively. During fast variations in the operational temperature, the maximum power that can be extracted from the fuel cell is increased. On the other hand, the P-I polarization curves with a constant operational temperature but different membrane water contents are shown

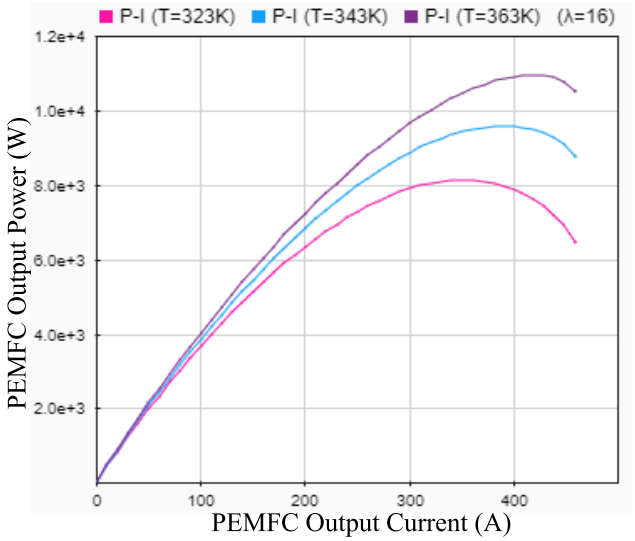

FIGURE 14. PEMFC P-I polarization curve with different operational temperature.

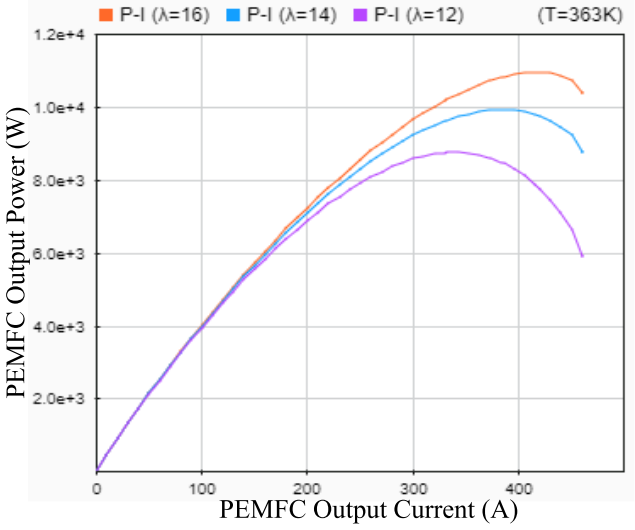

FIGURE 15. PEMFC P-I polarization curve with different operational temperature and membrane water content.

in Figure 15. When the membrane water contents are 16, 14, and 12 at a constant operational temperature ($T = 363K$), the maximum power points of the fuel cell are 10970 W, 9940 W, and 8765 W, respectively. Therefore, the maximum power of the fuel cell decreases when the membrane water content decreases.

Figure 16 shows the simulation result for the output power extracted from the PEMFC. The output power achieves the MPP within 0.015 s when the fuel cell operation is started. After that, the output power is increased at 0.5 s and 1.0 s due to the increase of operational temperature. Then, it is decreased at 2.0 s and 2.5 s due to the decrease of membrane water content. However, during the fast variation of the fuel cell parameter, the output power extracted by the fuel cell is slightly lower than the theoretical MPP, as shown in Figures 14 and 15. This is because the partial pressure of the reactance gases decreases with time, as discussed in the previous case. This simulation result shows that the proposed predictive MPPT technique is robust to parameter changes. It can track the new MPP of the PEMFC within 2 ms under a fast variation of the parameter.

C. SIMULATION WITH VARIABLE LOAD RESISTANCE

In this simulation, the PEMFC system still follows the parameters listed in Table 2, but there is a fast variation in the load resistance. This simulation aims to investigate the robustness of the proposed MPPT technique for load changes. The initial load resistance is 10 Ω. After 1 s, a parallel load with 10 Ω resistance is switched on. Therefore, the total resistance is decreased to 5 Ω. Another load with 1.25 Ω resistance is switched on at 2 s. The final total resistance is turned to 1 Ω. Figure 17 shows the simulation results for the output power extracted from the PEMFC.

The PEMFC system reaches the maximum output power with zero overshoot. Then, it maintains the maximum output power even though there is a fast variation in the load resistance. Therefore, there is sufficient evidence to prove that the proposed predictive MPPT technique is robust to load changes. Figures 18, 19, and 20 show the load voltage, current, and power consumed by the load. When the load resistance is decreased, the power consumed by the load is maintained at the maximum power produced by the PEMFC. However, there are changes in the load voltage, current, and power. The electrical circuit must fulfill Ohm's Law, $V = IR$ and the formula of power $P = VI$. Although the power absorbed by the load remains at the same value, the load voltage and current are changed because of the different resistances.

From Figures 18 and 19, the output voltage, V_o is changed from 290 V to 205 V and then to 91 V but the output current, I_o is increased from 29 A to 41 A and then to 91 A. In addition, there are two power transients, as shown in Figure 20. These power transient states occurred precisely when the parallel loads were switched on. This is because the sudden change in the total load resistance causes the load current to overshoot. A similar occurrence was also presented in [15].

At 1s, the total load resistance is changed from 10 Ω to 5 Ω, but the output voltage is not directly reduced from 290 V to 205 V. It takes approximately 0.2 s to regulate the output voltage because the capacitor in the DC-DC boost converter releases energy and slows down the voltage drop. During the output voltage regulation, the electrical circuit still follows Ohm's law. Therefore, when the total resistance suddenly decreases while the voltage is maintained at a high level, the changes will fall on the current.

The current waveforms in Figure 19 shows the output current is overshoot when the total load resistance changes from high to low. The current raised can be estimated from the ratio of the resistance changes. For example, when the load resistance changed from 10 Ω to 5 Ω at 1 s, the current increased by 2 times which from 29 A to 58 A. Furthermore, at 2 s, the load resistance changed from 5 Ω to 1 Ω, causing

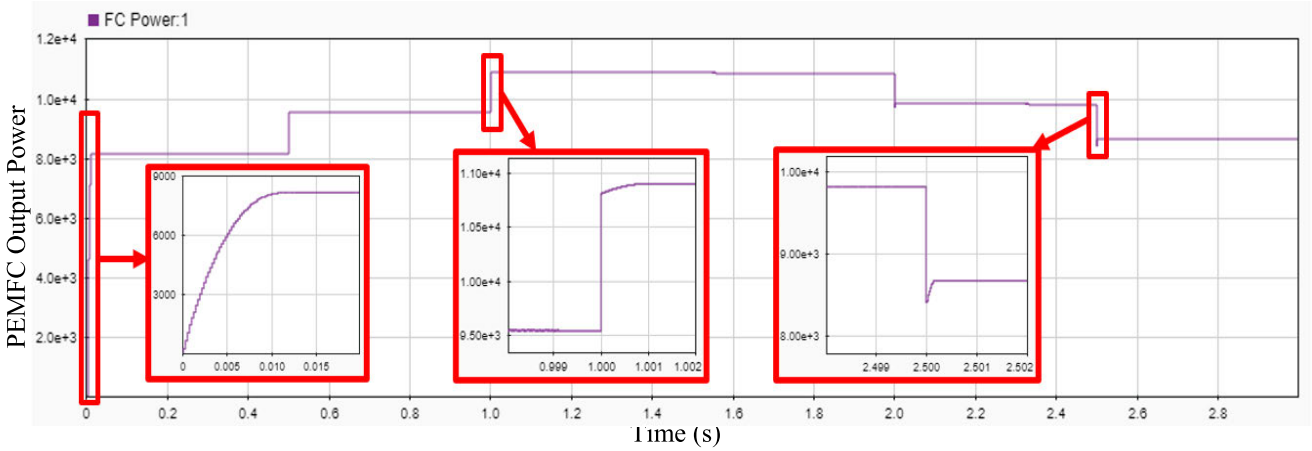

FIGURE 16. PEMFC output power with fast variation of operational temperature and membrane water content.

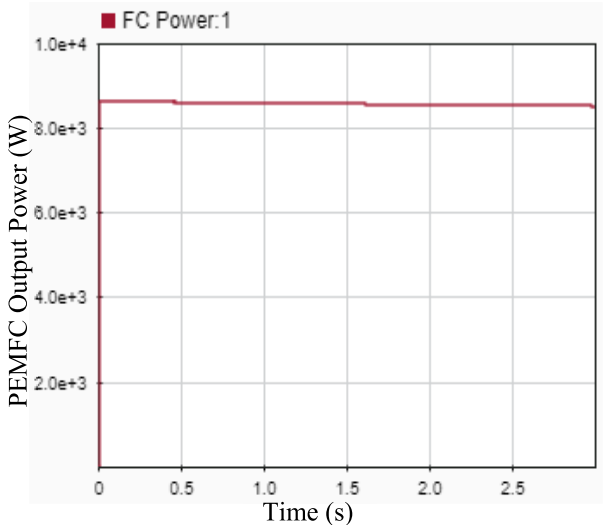

FIGURE 17. PEMFC output power with fast variation of load resistance.

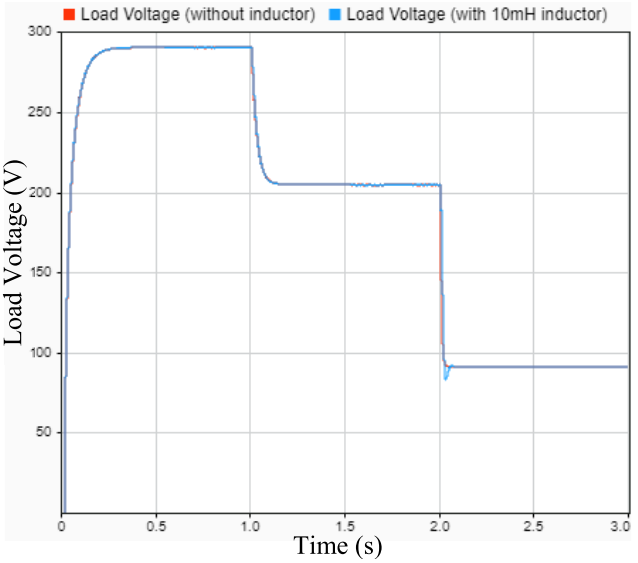

FIGURE 18. Load voltage with fast variation of load resistance.

the current to increase by five times. Therefore, the power transient at 2 s was much higher than the power transient at 1 s. However, if the load resistance changes from low to high, the current will be undershooting. It is concluded that this sudden change in the output current causes a power transient at the load side.

One of the ways to solve the overshooting problem is to include an inductor at the load side. The characteristic of the inductor is to prevent the rapid changes of electric current. This is because the inductor changes the electric current into the magnetic field. The magnetic field induces an electromotive force when there is changing in current flow. The electromotive force is the inductor voltage which has a polarity. It opposes any changes in current that flow through the inductor. Therefore, an inductor can be used to reduce the overshooting current. Figures 18, 19, and 20 also show the comparison results with a 10 mH inductor and without using the inductor. Figure 19 shows the overshooting current at 2 s is reduced from 200 A to 130 A when a 10mH inductor was used. Figure 20 also shows the overshooting power is reduced from 40 kW to 20 kW. It proves that the inductor can cut down the high power transient to half of the original value. This may protect the dc-dc converter when there is any changing of load resistance.

Another difference between the two power transients is the time taken for the load power to restore its steady state. At 1 s, the DC-DC boost converter takes 0.2 s to regulate the output voltage from 290V to 205V. However, it only takes 0.04 s to control the output voltage from 205 V to 91 V at 2 s. This shows that it is faster to achieve a steady state at 2 s. This is because the time constant for the capacitor to release energy is reduced based on the resistance. The equation for the capacitor discharge voltage can be expressed as:

$$V_C(t) = V_d \times e^{-\frac{t}{RC}} \tag{23}$$

where V_C is the capacitor voltage, V_d is the capacitor voltage to be discharged, R is the resistance value, and C is the

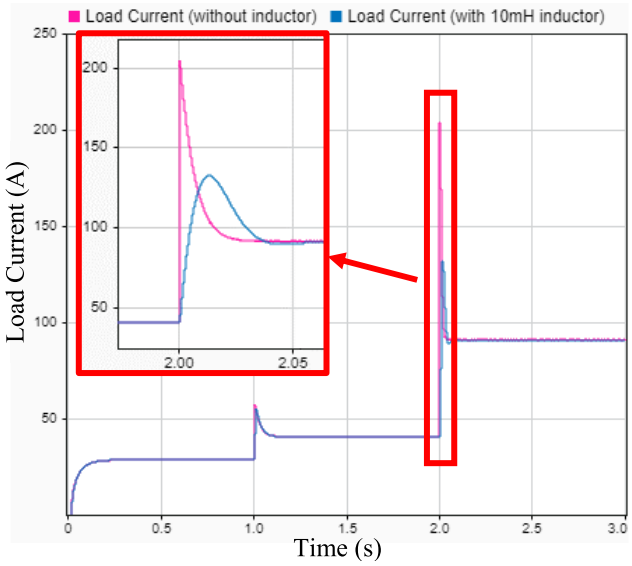

FIGURE 19. Load current with fast variation of load resistance.

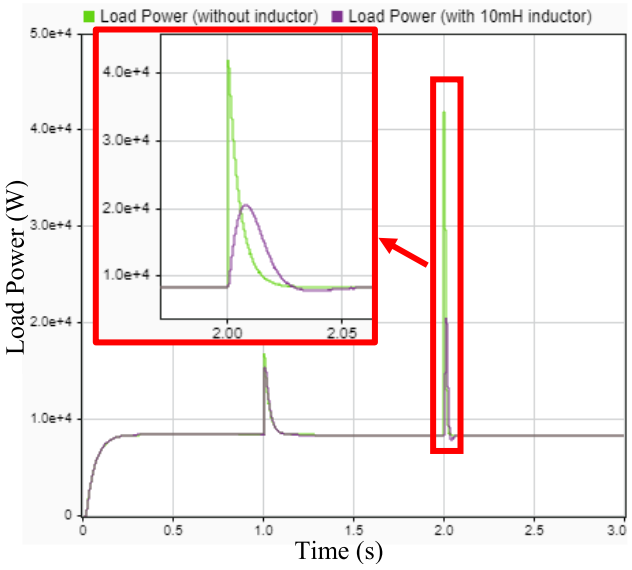

FIGURE 20. Load power with fast variation of load resistance.

capacitance value. The capacitor time constant is equal to the product of the resistance and capacitance value. Therefore, a lower resistance value will result in a lower capacitor time constant and cause the time to achieve the steady state to become faster.

V. CONCLUSION

In this study, a predictive MPPT technique is designed for a PEMFC system. The predictive MPPT technique is investigated by comparing its performance with that of other MPPT techniques. The results prove that the proposed predictive MPPT technique has the fastest MPP tracking time. Therefore, the proposed predictive MPPT technique exhibits the best performance when compared with the PSO-PID, P&O, and SMC-based MPPT methods. The predictive MPPT technique was validated by changing the fuel cell parameters and load resistance. It is confirmed that the predictive MPPT technique can lead the PEMFC system to reach the new MPP in a very short time. In conclusion, the proposed MPPT technique exhibits fast tracking of the MPP locus, outstanding accuracy, and robustness to the environmental changes.

REFERENCES

[1] N. Karami, L. E. Khoury, G. Khoury, and N. Moubayed, "Comparative study between P&O and incremental conductance for fuel cell MPPT," in *Proc. Int. Conf. Renew. Energies Developing Countries*, Nov. 2014, pp. 17–22, doi: 10.1109/REDEC.2014.7038524.

[2] V. Boscaino, R. Miceli, and G. Capponi, "MATLAB-based simulator of a 5 kw fuel cell for power electronics design," *Int. J. Hydrogen Energy*, vol. 38, no. 19, pp. 7924–7934, 2013, doi: 10.1016/j.ijhydene.2013.04.123.

[3] B. Gou, W. K. Na, and B. Diong, *Fuel Cell Modeling, Control, and Applications*. Boca Raton, FL, USA: Taylor & Francis, 2010, pp. 125–138.

[4] Z.-D. Zhong, H.-B. Huo, X.-J. Zhu, G.-Y. Cao, and Y. Ren, "Adaptive maximum power point tracking control of fuel cell power plants," *J. Power Sources*, vol. 176, no. 1, pp. 259–269, Jan. 2008, doi: 10.1016/j.jpowsour.2007.10.080.

[5] V. Karthikeyan, P. V. Das, and F. Blaabjerg, "Implementation of MPPT control in fuel cell fed high step up ratio DC-DC converter," in *Proc. 2nd IEEE Int. Conf. Power Electron., Intell. Control Energy Syst. (ICPEICES)*, Oct. 2018, pp. 689–693, doi: 10.1109/ICPEICES.2018.8897443.

[6] N. Naseri, S. E. Hani, A. Aghmadi, K. E. Harouri, M. S. Heyine, and H. Mediouni, "Proton exchange membrane fuel cell modelling and power control by P&O algorithm," in *Proc. 6th Int. Renew. Sustain. Energy Conf. (IRSEC)*, Dec. 2018, pp. 1–5, doi: 10.1109/IRSEC.2018.8703002.

[7] S. Dharani and R. Seyezhai, "Development of simulator and MPPT algorithm for PEM fuel cell," *Commun. Appl. Electron.*, vol. 2, no. 7, pp. 36–41, Aug. 2015, doi: 10.5120/cae2015651774.

[8] M. Dargahi, M. Rezanejad, J. Rouhi, and M. Shakeri, "Maximum power point tracking for fuel cell in fuel cell/battery hybrid systems," in *Proc. IEEE Int. Multitopic Conf.*, Dec. 2008, pp. 33–37, doi: 10.1109/INMIC.2008.4777703.

[9] D. Luta and A. Raji, "Fuzzy rule-based and particle swarm optimisation MPPT techniques for a fuel cell stack," *Energies*, vol. 12, no. 5, p. 936, Mar. 2019, doi: 10.3390/en12050936.

[10] J. Jiao and X. Cui, "Adaptive control of MPPT for fuel cell power system," *J. Converg. Inf. Technol.*, vol. 8, no. 4, pp. 362–371, Feb. 2013, doi: 10.4156/jcit.vol8.issue4.43.

[11] S. Abdi, K. Afshar, N. Bigdeli, and S. Ahmadi, "A novel approach for robust maximum power point tracking of PEM fuel cell generator using sliding mode control approach," *Int. J. Electrochem. Sci.*, vol. 7, no. 5, pp. 4192–4209, 2012.

[12] S. Ahmadi, S. Abdi, and M. Kakavand, "Maximum power point tracking of a proton exchange membrane fuel cell system using PSO-PID controller," *Int. J. Hydrogen Energy*, vol. 42, no. 32, pp. 20430–20443, Aug. 2017, doi: 10.1016/j.ijhydene.2017.06.208.

[13] M. Derbeli, O. Barambones, M. Farhat, and L. Sbita, "Efficiency boosting for proton exchange membrane fuel cell power system using new MPPT method," in *Proc. 10th Int. Renew. Energy Congr. (IREC)*, Mar. 2019, pp. 1–4, doi: 10.1109/IREC.2019.8754587.

[14] M. Derbeli, O. Barambones, and L. Sbita, "A robust maximum power point tracking control method for a PEM fuel cell power system," *Appl. Sci.*, vol. 8, no. 12, p. 2449, Dec. 2018, doi: 10.3390/app8122449.

[15] M. Derbeli, O. Barambones, M. Farhat, J. A. Ramos-Hernanz, and L. Sbita, "Robust high order sliding mode control for performance improvement of PEM fuel cell power systems," *Int. J. Hydrogen Energy*, vol. 45, no. 53, pp. 29222–29234, Oct. 2020, doi: 10.1016/j.ijhydene.2020.07.172.

[16] M. Z. Romdlony, B. R. Trilaksono, and R. Ortega, "Experimental study of extremum seeking control for maximum power point tracking of PEM fuel cell," in *Proc. Int. Conf. Syst. Eng. Technol. (ICSET)*, Sep. 2012, pp. 1–6, doi: 10.1109/ICSEngT.2012.6339313.

[17] K. J. Reddy and N. Sudhakar, "High voltage gain interleaved boost converter with neural network based MPPT controller for fuel cell based electric vehicle applications," *IEEE Access*, vol. 6, pp. 3899–3908, 2017, doi: 10.1109/ACCESS.2017.2785832.

[18] S. Srinivasan, R. Tiwari, M. Krishnamoorthy, M. P. Lalitha, and K. K. Raj, "Neural network based MPPT control with reconfigured quadratic boost converter for fuel cell application," *Int. J. Hydrogen Energy*, vol. 46, no. 9, pp. 6709–6719, Feb. 2021, doi: 10.1016/j.ijhydene.2020.11.121.

[19] A. Fathy, M. A. Abdelkareem, A. G. Olabi, and H. Rezk, "A novel strategy based on salp swarm algorithm for extracting the maximum power of proton exchange membrane fuel cell," *Int. J. Hydrogen Energy*, vol. 46, no. 8, pp. 6087–6099, Jan. 2021, doi: 10.1016/j.ijhydene.2020.02.165.
[20] H. Rezk, A. Fathy, and A. Y. Abdelaziz, "A comparison of different global MPPT techniques based on meta-heuristic algorithms for photovoltaic system subjected to partial shading conditions," *Renew. Sustain. Energy Rev.*, vol. 74, pp. 377–386, Jul. 2017, doi: 10.1016/j.rser.2017.02.051.
[21] A. Fathy and H. Rezk, "Multi-verse optimizer for identifying the optimal parameters of PEMFC model," *Energy*, vol. 143, pp. 634–644, Jan. 2018, doi: 10.1016/j.energy.2017.11.014.
[22] J. Rodriguez and P. Cortes, *Predictive Control of Power Converters and Electrical Drives*. Chichester, U.K.: Wiley, 2012, pp. 31–39.
[23] D. F. Pereira, F. da Costa Lopes, and E. H. Watanabe, "Neural generalized predictive control for tracking maximum efficiency and maximum power points of PEM fuel cell stacks," in *Proc. 44th Annu. Conf. IEEE Ind. Electron. Soc. (IECON)*, vol. 1, Oct. 2018, pp. 1878–1883, doi: 10.1109/IECON.2018.8591290.
[24] M. Derbeli, A. Charaabi, O. Barambones, and C. Napole, "High-performance tracking for proton exchange membrane fuel cell system pemfc using model predictive control," *Mathematics*, vol. 9, no. 11, pp. 1–17, 2021, doi: 10.3390/math9111158.
[25] F. Musio, F. Tacchi, L. Omati, P. Gallo Stampino, G. Dotelli, S. Limonta, D. Brivio, and P. Grassini, "PEMFC system simulation in MATLAB-Simulink environment," *Int. J. Hydrogen Energy*, vol. 36, no. 13, pp. 8045–8052, Jul. 2011, doi: 10.1016/j.ijhydene.2011.01.093.
[26] S. Chugh, C. Chaudhari, K. Sonkar, A. Sharma, G. S. Kapur, and S. S. V. Ramakumar, "Experimental and modelling studies of low temperature PEMFC performance," *Int. J. Hydrogen Energy*, vol. 45, no. 15, pp. 8866–8874, Mar. 2020, doi: 10.1016/j.ijhydene.2020.01.019.
[27] E. W. Saeed and E. G. Warkozek, "Modeling and analysis of renewable PEM fuel cell system," *Energy Proc.*, vol. 74, pp. 87–101, Aug. 2015, doi: 10.1016/j.egypro.2015.07.527.
[28] I. Soltani, "An intelligent, fast and robust maximum power point tracking for proton exchange membrane fuel cell," *World Appl. Program.*, vol. 3, pp. 264–281, Jul. 2013.
[29] L. Cheng, P. Acuna, R. P. Aguilera, M. Ciobotaru, and J. Jiang, "Model predictive control for DC-DC boost converters with constant switching frequency," in *Proc. IEEE 2nd Annu. Southern Power Electron. Conf. (SPEC)*, Dec. 2016, pp. 1–6, doi: 10.1109/SPEC.2016.7846189.
[30] S. Palanidoss and T. V. S. Vishnu, "Experimental analysis of conventional buck and boost converter with integrated dual output converter," in *Proc. Int. Conf. Electr., Electron., Commun., Comput., Optim. Techn. (ICEECCOT)*, Dec. 2017, pp. 323–329, doi: 10.1109/ICEECCOT.2017.8284521.

JYE YUN FAM was born in Sarawak, Malaysia, in 1995. He received the B.Eng. degree in electrical and electronics engineering from Universiti Malaysia Sarawak (UNIMAS), Malaysia, in 2019, where he is currently pursuing the master's degree with the Department of Electrical and Electronics Engineering.

His research interest includes energy efficiency of renewable energy.

SHEN YUONG WONG (Senior Member, IEEE) received the bachelor's and master's degrees (Hons.) in electrical and electronic engineering and the Ph.D. degree in engineering from Universiti Tenaga Nasional (the National Energy University), Malaysia.

She is currently an Associate Professor with the Department of Electrical and Electronics Engineering, Xiamen University Malaysia. Her research interests include power system fault detection and diagnosis, extreme learning machine, classification, regression, and other applications of artificial intelligence. She is a Professional Engineer (P.Eng.) registered to the Board of Engineers Malaysia (BEM), accredited under the Washington Accord. She serves as an editorial board member for several journals.

HAZRUL BIN MOHAMED BASRI (Member, IEEE) was born in Perak, Malaysia, in 1984. He received the B.Eng. degree from the Université de Technologie de Belfort Montbéliard, France, in 2010, and the Ph.D. degree from Universiti Malaya, Malaysia, in 2019.

He is currently a Senior Lecturer with the Faculty of Engineering, Universiti Malaysia Sarawak, Malaysia. His research interests include power electronics, renewable energy, and multi-objective optimization algorithm.

Dr. Mohamed Basri is a Registered Professional Engineer from the Board of Engineers, Malaysia.

MOHAMMAD OMAR ABDULLAH received the B.Eng. and M.Sc. degrees in petroleum and natural gas engineering from Universiti Teknologi Malaysia (UTM), in 1989 and 1991, respectively, and the Ph.D. degree from the University of Hertfordshire (UH), U.K., in 2002.

He has been a Professor of applied energy and environment at the Department of Chemical Engineering and Energy Sustainability (ChemES), Faculty of Engineering, Universiti Malaysia Sarawak (UNIMAS), since 2014. He is currently the Founding Head of ChemES, UNIMAS. He is the Co-Owner of OSYIHM Farm, a non-pesticide farm promoting clean hybrid energy use and supporting integrated healthy and sustainable farming. His strength is indicated by his industrial-related research on applied energy and environment. He was appointed as a Senior Member of the Academy of Malaysian SMEs (S.M.A.M.S), in March 2009, during the IKS2009 Presentation and Exhibition, Putra World Trade Center, Kuala Lumpur. He has been a Registered Member of IMechE and a Charted Engineer (C.Eng.) of U.K., since September 2004. He has been a member of the American Society of Heating Refrigeration and Air-Conditioning Engineers (ASHRAE), since August 2004.

KASUMAWATI BINTI LIAS (Member, IEEE) was born in Sarawak, Malaysia, in 1981. She received the M.Eng. degree from Universiti Teknologi Malaysia, Malaysia, in 2008, and the Ph.D. degree from Universiti Teknologi MARA, Malaysia, in 2020.

She is currently a Lecturer with the Faculty of Engineering, Universiti Malaysia Sarawak, Malaysia. Her research interest includes biomedical engineering.

Dr. Lias is a Registered Professional Engineer from the Board of Engineers, Malaysia.

SAAD MEKHILEF (Senior Member, IEEE) is currently a Distinguished Professor at the School of Science, Computing and Engineering Technologies, Swinburne University of Technology, Australia, and an Honorary Professor at the Department of Electrical Engineering, University of Malaya, Malaysia. He has authored and coauthored more than 400 publications in academic journals and proceedings and five books with more than 31,000 citations. He is actively involved in industrial consultancy for major corporations in power electronics projects. His research interests include power conversion techniques, control of power converters, renewable energy, and energy efficiency. He is an IET Fellow. He is an Associate Editor of IEEE Transactions on Power Electronics and *Journal of Power Electronics*.